Food Chemistry: X 16 (2022) 100485

Contents lists available at ScienceDirect

Food Chemistry: X

journal homepage: www.sciencedirect.com/journal/food-chemistry-x

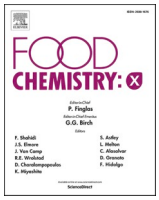

The flavor profile changes of Pacific oysters (*Crassostrea gigas*) in response to salinity during depuration

Lipin Chen [a], Hongwei Zhang [c], Haohao Shi [a,b,*], Changhu Xue [a,d], Qi Wang [a], Fanqianhui Yu [a], Yong Xue [a], Yuming Wang [a], Zhaojie Li [a,d,*]

[a] College of Food Science and Engineering, Ocean University of China, No.5, Yu Shan Road, Qingdao, Shandong Province 266003, PR China
[b] College of Food Science and Technology, Hainan University, Hainan 570228, PR China
[c] Food and Agricultural Products Testing Agency, Technology Center of Qingdao Customs District, Qingdao, Shandong Province 266237, PR China
[d] Collaborative Innovation Center of Seafood Deep Processing, Dalian Polytechnic University, Dalian 116034, PR China

ARTICLE INFO

Keywords:
Salinity
Flavor
Taste
Odor
Pacific oyster (*Crassostrea gigas*)
Depuration

ABSTRACT

The effect of salinity on taste and odor characteristics of Pacific oyster (*Crassostrea gigas*) during depuration was investigated in this study. In combination with free amino acids (FAAs), 5'-nucleotides, and organic acids, electronic tongues were measured to evaluate the changes in taste-related compounds. Gas chromatography-ion mobility spectrometry (GC-IMS) and electronic nose were used to analyze the odor compounds of *C. gigas* at different depuration salinities. The results showed that bitter substances in *C. gigas* significantly decreased as salinity decreased. The equivalent umami concentration (EUC) was highest at a salinity of 29 g/L. The GC-IMS results were consistent with the electronic-nose test results. After low-salinity depuration, aldehyde and ketone levels were significantly reduced, and furan concentrations increased. In addition, multivariate analysis was used to determine the correlation between each component and flavor profile differences due to depuration at various salinities. Overall, salinity of 29 g/L could be optimal for oyster depuration.

Introduction

The Pacific oyster (*Crassostrea gigas*) is a bivalve mollusk with high nutritional value and rich flavor compounds, making it popular worldwide (Chen et al., 2020). According to the Food and Agriculture Organization, the global aquaculture production of *C. gigas* in 2018 totaled 643.5 thousand tons (FAO, 2020). They are mainly eaten raw or lightly heated to avoid losing flavor during processing. To ensure the ingestible safety of raw Pacific oyster, depuration, a process that involves keeping oyster in sterile seawater for >48 h (Anacleto et al., 2015), has emerged as one of the greatest mechanisms of processing. Salinity is a key environmental factor in the depuration process because it affects the total number of oyster colonies, as well as their mortality and physiological processes (Bagenda et al., 2019). Seawater salinity is also known to play a significant role in the flavor traits of seafood (Bi et al., 2021; Zhang, Yin, Zheng, Xu, et al., 2021). The umami taste of seafood can be improved by maintaining salinity within a certain range. In a study by Bi et al. (2021), it was found that seawater salinity influenced the content of taste-related compounds in Pacific oysters, and 28 g/L salinity was the optimal salinity acceptable to consumers. Zhang, Yin, Zheng, Tao, et al. (2021) improved the taste quality (which is affected by 5'-nucleotides and free amino acids (FAAs)) of *Eriocheir sinensis* by temporarily rearing them in saltwater post-harvest. However, the effect of salinity on the flavor traits of Pacific oysters during depuration remains unclear.

Flavor, which is a combination of taste and odor, is an important factor that directly affects customer choices (Feng et al., 2022). Taste is mainly recognized by taste receptors in the taste buds of the tongue and palate epithelium by detecting non-volatile compounds such as those producing acid, fresh, bitter, and salty flavors. These non-volatile compounds are mainly derived from secondary metabolites including FAAs and organic acids (Tian et al., 2020; Li et al., 2021). Currently, the equivalent umami concentration (EUC), electronic tongues, and sensory evaluation are mainly used to evaluate taste characteristics. Odors are derived from different types of volatile organic compounds (VOCs), including esters, *N*-containing compounds, alcohols, and ketones (Feng, Ng, Mikś-Krajnik, & Yang, 2017), which can be evaluated by electronic noses and gas chromatography-ion mobility spectrometry (GC-IMS) (Duan, Dong, Dong, et al., 2021). An electronic nose can simulate the

* Corresponding authors at: Haikou 570228, Hainan, PR China (H. Shi). Qingdao 266003, Shandong, PR China (Z. Li).
E-mail addresses: shihaohao@hainanu.edu.cn (H. Shi), lizhaojie@ouc.edu.cn (Z. Li).

https://doi.org/10.1016/j.fochx.2022.100485
Received 17 May 2022; Received in revised form 18 October 2022; Accepted 19 October 2022
Available online 20 October 2022
2590-1575/© 2022 The Authors. Published by Elsevier Ltd. This is an open access article under the CC BY-NC-ND license (http://creativecommons.org/licenses/by-nc-nd/4.0/).

biological olfactory system and analyze a smell as an overall odor difference at high speed and low cost. GC-IMS is a novel method for analyzing VOCs that combines GC with IMS to quickly identify substances. According to previous studies, the majority VOCs of aquatic products are formed by oxidation (Hu, Wang, Liu, Cao, & Xue, 2021). However, the correlation between taste and odor has yet to be elucidated. At present, bidirectional orthogonal partial least squares (O2PLS) is a new statistical tool with the capability to analyze two types of data (x/y) simultaneously. It has been used to analyze the correlation between microbiota succession and flavor formation in *Cyprinus carpio* L. during fermentation (Zang et al., 2020). Other chemometric tools, such as principal component analysis (PCA), orthogonal partial least squares (OPLS-DA), shared and unique structure (SUS-plot), and bidirectional orthogonal partial least squares (O2PLS), are also used to further analyze data (Abdul Ghani, Husin, Rashid, Shaari, & Chik, 2016; Boccard et al., 2011; Zhao et al., 2021).

The flavor traits of *C. gigas* at different salinities (26, 29, 32, 35, and 38 g/L) during depuration were investigated in this study using: 1) electronic tongue technology to evaluate the overall taste differences and changes in taste components of Pacific oysters, and FAAs, nucleotides, and organic acids; 2) GC-IMS and electronic nose to establish the fingerprints of VOCs; and 3) chemometric approaches, including PCA, OPLS-DA, O2PLS, and SUS-plot, to analyze the data and screen out flavor change markers.

Materials and methods

Sample preparation and chemicals

C. gigas samples with an average weight of 112 g were collected from a farm in Qingdao (Shandong Province, 36°16′49″N, 120°00′36″E), China, and transported quickly (<1.5 h) on ice to the Ocean University of China Laboratory (Qingdao, Shandong Province, China) in April 2021. After the samples were washed, before depuration, 15 live samples were selected as the control group (sample code: Pro-depuration), and 200 live samples were randomly selected for depuration according to a regulatory procedure (Chen et al., 2021a). *C. gigas* were placed in five depuration tanks containing artificial seawater, fitted with ozone radiation (0.4 mg/L) and ultraviolet (UV) systems, and the temperature was controlled at 15 °C. The one group of salinity was set at 32 g/L (consistent with the Pacific oyster production area, sample code: S32), while the other four groups were set as 26 g/L (S26), 29 g/L (S29), 35 g/L (S35), and 38 g/L (S38). After depuration for 72 h, 15 individuals were selected from each salinity group. Of these, five individuals were combined into one test sample. The soft tissues were quickly separated from the shells, homogenized, and then stored at −80 °C.

Hydrochloric acid (HCl), sulfosalicylic acid, potassium hydroxide (KOH), ammonium dihydrogen phosphate ($NH_4H_2PO_4$), perchloric acid ($HClO_4$), citric acid, acetic acid, and triethylamine were purchased from Sinopharm Chemical Reagent Company (Shanghai, China). Standard compounds (5′-nucleotides and organic acids) were purchased from Sigma-Aldrich (St. Louis, MO, USA).

Taste components analysis

Electronic tongue analysis

The taste traits of *C. gigas* were analyzed using an electronic tongue (TS-5000Z, Intelligent Sensor Technology, Inc., Atsugi, Japan) (Tian et al., 2020). The electronic tongue was equipped with an artificial lipid membrane sensor with a wide area selection specificity to simulate the taste perception mechanism of living organisms. Thirty grams of each sample were homogenized with 150 mL of distilled water (10000 rpm, 60 s) and then centrifuged (1500 × *g*, 10 min, 4 °C). Each sample was cycled four times. The device measured the saltiness, bitterness, astringency, sourness, and umami of the samples by detecting changes in the membrane potential caused by electrostatic or hydrophobic interactions between various taste-related substances and artificial lipid membranes. After a short sensor cleaning procedure (2 × 3 s), aftertaste A (bitter aftertaste), aftertaste B (astringency aftertaste), and richness (umami aftertaste) intensities were measured. The results were analyzed using the TS-5000Z Library search software (Intelligent Sensor Technology, Inc., Atsugi, Japan).

Analysis of FAAs

The FAAs were extracted according to a previously described protocol (Bi et al., 2021). Samples (5 g) were homogenized in 10 mL of dilute HCl (0.20 M) and centrifuged (13,000 × *g*, 10 min, 4 °C). The supernatant was then diluted to a volume of 25 mL. Two milliliters of 5 % sulfosalicylic acid were added to 2 mL of diluent and then the mixture was centrifuged (10,000 × *g*, 4 °C, 10 min). The supernatant was filtered through 0.22 μm filters (Agilent Technologies Inc., Santa Clara, CA, USA) and analyzed using an automatic amino acid analyzer (L-8900, Hitachi, Tokyo, Japan).

Analysis of 5′-nucleotides and organic acids

To analyze 5′-nucleotides, 5 g of the sample was homogenized with 15 mL of 10 % perchloric acid and then centrifuged at 12,000 × *g* for 15 min at 4 °C. The supernatant was neutralized using two KOH solutions (10 M and 1 M, respectively), diluted to 25 mL, and then stored at − 80 °C.

The 5′-nucleotides in the samples were separated using a high-performance liquid chromatography (HPLC) (Agilent Technologies Inc., Santa Clara, CA, USA) equipped with a CAPCELLPAK C18 SG column (4.6 mm × 150 mm, Shiseido Co., ltd., Tokyo, Japan) (Chen et al., 2021b; Zhao, Wu, Chen, & Yang, 2019) equilibrated with a mixture of 20 mM citric acid, 20 mM acetic acid, and 40 mM triethylamine (pH 4.8) in isocratic mode at a flow rate of 0.8 mL/min. The column temperature was 40 °C, and the detector wavelength was 260 nm.

To determine organic acid levels, 5 g of sample was homogenized with 30 mL of 2.0 % $NH_4H_2PO_4$ and then centrifuged at 12,000 × *g* for 15 min at 4 °C. The supernatant was combined and diluted in a 50 mL volumetric flask. The supernatant was filtered through a 0.22 μm syringe filter and analyzed using HPLC with a C18 column (4.6 × 150 mm, Shiseido Co., ltd., Tokyo, Japan) equilibrated with 2.0 % $NH_4H_2PO_4$ (pH 2.9). The elution was monitored using UV absorption at 205 nm. The flow rate was set at 1 mL/min (Chen et al., 2021a).

The 5′-nucleotides and organic acids were identified by comparing the retention times of their HPLC peaks with those of standard compounds. An external standard method was used for quantization. Calibration curves were established based on the peak areas of the standard compounds.

EUC analysis

The EUC was defined as the concentration of monosodium glutamate (MSG) equivalent required for umami taste, which reflects the contribution of umami amino acids (aspartic acid (Asp) and glutamic acid (Glu)) and 5′-nucleotides (5'-inosine monophosphate (IMP), 5'-guanosine monophosphate (GMP), and 5'-adenosine monophosphate (AMP)) (Bi et al., 2021). It was calculated as follows: $EUC = a_i b_i + 1218\ (a_i b_i)(a_j b_j)$, where a_i is the amino acid (Asp or Glu) concentration (g/100 g), b_i is the relative umami concentration of umami amino acids (Glu, 1 and Asp, 0.077), a_j is the nucleotide (5′-IMP, 5′-GMP, 5′-AMP) concentration (g/100 g), b_j is the relative umami concentration for nucleotides (IMP, 1; GMP, 2.3; and AMP, 0.18), and 1218 is a synergistic constant.

Sensory evaluation

Sensory evaluation was performed according to the methods described by Bi et al. (2021) and Tian et al. (2020). The definitions of the sensory attributes are listed in Table S1, as described by Yao et al. (2018), and the reference samples were purchased from the Qidong market (Qingdao, China). Participants (n = 10, 50 % women and 50 % men, aged 27–55 years) were selected from the Ocean University of

China after training. After washing, the Pacific oysters were shelled and placed in a plastic cup (coded with a 3-digit random code) and immediately served to sensory evaluators at room temperature (24–26 °C). Simultaneously, sensory reference oysters were steamed and provided along with the samples. The participants were asked to chew and swallow the sample and then give scores ranging from 1 to 5. The scales were used to rate the intensity of sensory attributes: 5-very strong, 4-strong, 3-normal, 2-weak, and 1-very weak (Kawabe, Murakami, Usui, & Miyasaki, 2019). There were 60 Pacific oyster samples and 10 panelists, and each panelist tasted six half-shell oysters (Pro-depuration, S26, S29, S32, S35, and S38). To avoid bias, panelists were required to take a 5 min break and wash their mouths with mineral water before tasting the next sample. The average of the scores assigned by the 10 panelists was used as the final evaluation score for each Pacific oyster group.

Prior to sensory evaluation, informed consent was obtained from participants and the privacy rights of human subjects were observed. The study was approved by the guidelines of the Ethical Committee of the College of Food Science and Engineering of the Ocean University of China (approval no. SPXY2021050210).

Odor components analysis

Electronic nose

An electronic nose (PEN-3, Airsense Technology Co., ltd., Germany) was used to analyze *C. gigas* samples and consisted of 10 metal oxide sensors with specific recognition of different volatile compounds: W1C: aromatic compounds; W1W: sulfur compounds, terpenes; W1S: methane, broad range of compounds; W2W: aromatics and organic sulfur compounds; W2S: broad range, alcohols; W3S: methane and aliphatic compounds; W3C: ammonia, aromatic compounds; W5S: nitrous oxides; W5C: alkanes and aromatics; and W6S: hydrocarbons (Hu et al., 2021; Huang et al., 2019). Data were analyzed using linear discriminant analysis (LDA).

GC-IMS analysis

The VOCs in *C. gigas* depurated at different salinities were analyzed using GC-IMS (FlavourSpecR, Dortmund, Germany) with an FS-SE-54-CB capillary column (15 m × 0.53 mm) at 40 °C (Duan, Dong, Sun, et al., 2021; Hu et al., 2021). Samples (1.50 g) were placed in a 20 mL headspace injection bottle and incubated at 60 °C (500 rpm, 20 min). Nitrogen (99.99 % purity) was used as the carrier gas at the following rate: 2 mL/min for 5 min, 100 mL/min for 5 min, and 150 mL/min for 7 min. The molecules were ionized in an IMS ionization chamber containing a tritium ionization source. When determining VOCs, *n*-ketones C4–C8 were used as external references to calculate the retention index (RI), and VOCs were identified by comparing the RI and drift time (DT) with the GC × IMS Library Search.

Data analysis

Samples were analyzed in triplicate for FAAs, nucleotides, and organic acids. The data are expressed as mean ± standard deviation (*S. D.*) and obeyed assumptions of normality and homogeneity of variance (data not shown). To analyze the significant differences in these indicators, one-way ANOVA was performed using the Statistical Product and Service Solutions (SPSS) statistical software (version 20.0, IBM, Chicago, IL, USA), followed by the least significant difference (LSD) test, with a statistical significance cut-off of $P < 0.05$. To identify the major markers of flavor change after depuration, a supervised OPLS-DA method was performed using SIMCA + software (version 16.0, Umetrics, Umeå, Sweden) with the following filtering criteria: variable importance in projection (VIP) value >1.0, $|p[\mathrm{corr}]|$ presented in the *S*-plot > 0.7 as well as $P < 0.05$ (Zhang et al., 2019). Furthermore, SUS-plots were used to synthesize the loadings of the two OPLS-DA models to screen out the flavor-changing substances whose production was caused by salinity stress. Specifically, the SUS-plot showed a correlation with the predictive component $|p(corr)|$ of the higher-salinity depurations (S35 and S38) *vs* Cont. (S32) (Model 1) on the x-axis, and lower-salinity depurations (S26 and S29) *vs* Cont. (S32) (Model 2) on the y-axis (Boccard et al., 2011). In addition, O2PLS was used to determine the association between taste and odor, in which taste data of *C. gigas* (defined as X matrix) were mapped to odor data (defined as Y matrix). Correlations were calculated using MetScape 3 and verified using hierarchical clustering analysis (HCA) (Zhang et al., 2019).

Results and discussion

Change in taste-related compounds of Pacific oysters at different salinities during depuration

Electronic tongue response

The relationship between the overall taste attributes obtained from the electronic tongue and *C. gigas* samples depurated at different salinities was analyzed using PCA (Fig. 1A). As shown in Fig. 1A, a progressive change along the first principal component (PC1) was observed from the left to the right part of the plot as salinity increased, indicating that salinity had a consistent effect on *C. gigas* flavor. Based on tasteless point evaluation, umami, bitterness, astringency, saltiness, and richness were selected to show the changes in taste-related compounds present in *C. gigas* that resulted from depuration at different salinities (Fig. 1B) (Xu et al., 2022). The corresponding intensities of sourness, aftertaste A (bitterness aftertaste), and aftertaste B (astringency aftertaste) were below the tasteless point, so they were not considered to have contributed, and the data are not shown. The bitterness of the S32 and Pro-depuration groups was the closest together, indicating that depuration had little effect on the bitterness of *C. gigas* under the same salinity conditions (Fig. 1B). The saltiness, bitterness, and astringency of the *C. gigas* depurated at different salinities were similar, with S38 having the largest value, followed by S35 and S29. S26 had the lowest values for both bitter and astringent tastes. The umami value of S29 was higher than that of the other salinity groups. These results showed that depuration salinity had an impact on the taste components of *C. gigas*, and the specific changes in components were analyzed in later experiments. These differences in taste might be attributable to the physiological and biochemical changes caused by salinity adaptation (Bi et al., 2021). Studies have also reported that an electronic tongue could be used to analyze taste differences caused by salinity changes in *Salmo salar*, which is consistent with our results (Duan, Dong, Sun, et al., 2021).

Analysis of FAAs

The type and level of FAAs endow *C. gigas* with unique flavor characteristics. In this study, the production of FAAs at different salinities during depuration was analyzed, and a total of 16 taste-active FAAs were detected in *C. gigas* samples, including umami FAAs (aspartic acid (Asp), glutamic acid (Glu)), sweet FAAs (threonine (Thr), serine (Ser), glycine (Gly), alanine (Ala), arginine (Arg), and proline (Pro)), bitter FAAs (valine (Val), methionine (Met), isoleucine (Ile), leucine (Leu), tyrosine (Tyr), phenylalanine (Phe), lysine (Lys), and histidine (His)), accounting for approximately 25 %, 60 %, and 15 % of total FAAs, respectively (Table 1) (Cochet, Brown, Kube, Elliott, & Delahunty, 2015; Yuasa et al., 2018). After depuration, the total FAA content in *C. gigas* showed a downward trend in the low-salinity groups (S26 and S29), which might have been caused by the stress consumption of FAAs during the depuration process. Asp and Glu are MSG-like components that impart an umami taste to food. As shown in Table 1, the Asp content was lower than that of Glu. The Asp and Glu levels of S29 were higher than those of the other groups. The levels of sweet FAAs showed an upward trend with increasing salinity and significantly increased in S38 ($P < 0.05$). We speculated that short-term high-salinity stress would lead to an increase in FAAs content, such as Ala, Thr, Gly, and Pro, which is consistent with previous research results (Hosoi, Kubota, Toyohara,

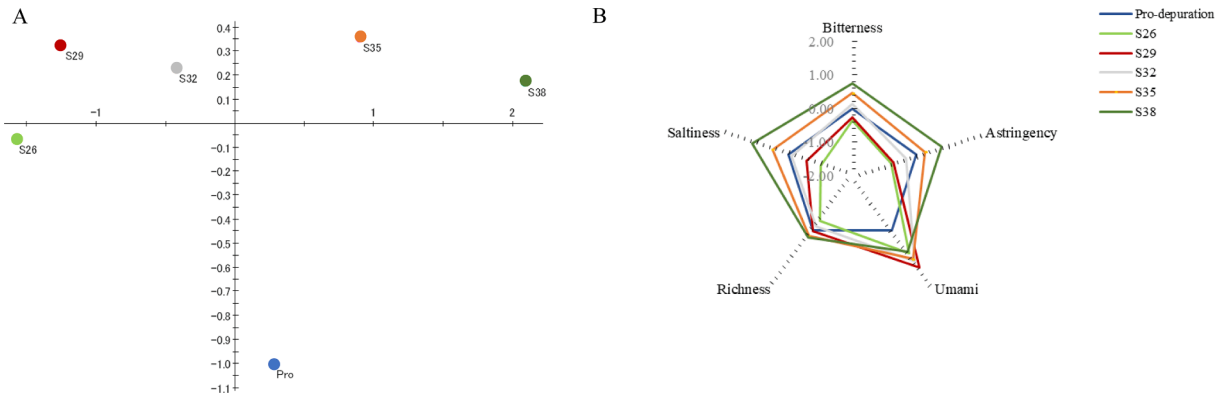

Fig. 1. (A) Principal component analysis (PCA) and (B) Spider plot for the electronic tongue sensory score based on the taste sensing system for Pacific oysters (*Crassostrea gigas*) depurated at different salinities. The data were analyzed using a TS-5000Z electronic tongue (INSENT, Japan) with wide-area selection-specific artificial lipid membrane sensors. Initial taste: bitterness, astringency, umami, saltiness, aftertaste: richness. Control (Pro-depuration) was represented as standard and its taste features were calculated as '0' by sensor response output.

Table 1
The content of free amino acids (FAAs), 5′-nucleotides, and organic acids of *Crassostrea gigas depurated* at different salinities.

		Content (FAAs, flavor nucleotides, organic acid mg/100 g, mean ± SD)					
		Pro-depuration	S26	S29	S32	S35	S38
FAAs	Asp	71.98 ± 4.26a	67.82 ± 4.05ab	68.65 ± 5.49ab	63.20 ± 8.37b	63.96 ± 3.53b	45.57 ± 4.01c
	Glu	113.67 ± 7.09a	110.02 ± 8.19a	111.17 ± 2.39a	101.44 ± 8.02b	100.43 ± 7.28b	92.04 ± 6.09c
	UFAAs	185.57 ± 6.35a	177.84 ± 9.24b	179.82 ± 8.51ab	164.64 ± 9.39c	164.39 ± 8.81c	137.61 ± 7.10e
	Thr	18.46 ± 1.57	17.12 ± 1.01	18.56 ± 1.08	19.57 ± 2.82	19.86 ± 7.63	20.71 ± 1.34
	Ser	29.55 ± 4.72 cd	32.27 ± 2.25bc	40.59 ± 3.15a	34.56 ± 3.41b	28.08 ± 2.88 cd	25.86 ± 1.66d
	Gly	102.46 ± 7.73a	47.22 ± 3.21c	75.08 ± 4.82b	91.45 ± 3.77ab	100.53 ± 9.13a	101.21 ± 8.99a
	Ala	83.81 ± 6.54c	68.08 ± 5.69c	86.12 ± 3.04c	107.98 ± 8.90b	133.12 ± 8.66a	148.94 ± 5.51a
	Arg	81.20 ± 7.55	77.11 ± 6.12	71.07 ± 5.74	73.08 ± 7.41	74.21 ± 6.72	68.84 ± 5.49
	Pro	122.72 ± 9.13b	104.13 ± 8.13c	110.38 ± 8.66bc	122.93 ± 5.26b	110.43 ± 7.94bc	149.81 ± 6.75a
	SFAAs	438.23 ± 19.16b	345.93 ± 21.41d	401.83 ± 24.49bc	449.57 ± 27.57b	466.21 ± 39.96b	515.36 ± 43.74a
	Val	11.40 ± 0.82ab	9.12 ± 0.77b	10.34 ± 0.53b	13.26 ± 1.22a	10.91 ± 2.26b	11.17 ± 1.00ab
	Met	13.36 ± 1.44ab	9.99 ± 1.93c	10.75 ± 0.41bc	12.99 ± 1.25ab	14.04 ± 3.98ab	15.79 ± 0.86a
	Ile	12.86 ± 1.04	11.04 ± 1.14	11.38 ± 0.82	13.82 ± 0.92	12.41 ± 1.18	12.83 ± 1.11
	Leu	17.24 ± 1.87	13.58 ± 1.24	14.17 ± 0.79	18.06 ± 1.48	15.55 ± 1.31	16.11 ± 1.22
	Tyr	17.62 ± 1.62a	11.81 ± 1.57b	14.90 ± 0.74ab	17.79 ± 1.03a	16.26 ± 1.20ab	16.86 ± 0.97a
	Phe	10.21 ± 1.63ab	7.04 ± 0.46b	7.31 ± 0.88ab	10.97 ± 1.33a	9.57 ± 0.50ab	10.62 ± 0.86ab
	Lys	17.78 ± 1.22	17.49 ± 1.14	18.73 ± 1.52	23.42 ± 0.93	23.58 ± 1.52	19.89 ± 1.35
	His	14.26 ± 1.33ab	11.64 ± 1.33b	12.22 ± 0.37b	16.47 ± 1.02a	17.65 ± 1.12a	17.00 ± 1.34a
	BFAAs	114.73 ± 10.57ab	91.71 ± 8.78b	99.80 ± 5.26b	126.78 ± 12.25a	119.97 ± 12.67ab	120.27 ± 7.71ab
	TFAAs	738.53 ± 51.69ab	615.48 ± 42.45c	681.45 ± 40.06b	740.99 ± 49.96ab	750.57 ± 50.99ab	773.24 ± 62.74a
Organic acids	Succinic acid	23.66 ± 2.05a	19.35 ± 1.68ab	24.77 ± 1.95a	16.60 ± 1.13b	24.11 ± 1.51a	17.78 ± 1.92b
	Lactic acid	0.27 ± 0.01ab	0.28 ± 0.01ab	0.26 ± 0.02ab	0.24 ± 0.02b	0.26 ± 0.01ab	0.31 ± 0.03a
Nucleotides	Hx	19.68 ± 1.58a	14.64 ± 0.91c	14.79 ± 0.37c	14.78 ± 0.02c	13.77 ± 0.26c	17.15 ± 0.81b
	AMP	25.20 ± 2.76bc	22.59 ± 0.70c	45.81 ± 3.96a	45.91 ± 3.31a	47.19 ± 0.99a	43.18 ± 0.75a
	IMP	3.54 ± 0.72c	2.51 ± 0.19d	5.59 ± 0.06b	4.79 ± 0.13bc	6.32 ± 0.12a	5.79 ± 0.27b
	GMP	10.23 ± 1.10b	11.04 ± 0.29b	13.01 ± 1.59a	12.49 ± 1.92ab	12.01 ± 1.37ab	13.38 ± 1.23a
EUC (g MSG/100 g)		4.50 ± 0.38c	4.60 ± 0.32c	6.22 ± 0.71a	5.38 ± 0.17b	5.64 ± 0.32b	5.01 ± 0.56b

Means with different letters within a column are significantly different ($P < 0.05$). Asp, aspartic acid; Glu, glutamic acid; Thr, threonine; Ser, serine; Gly, glycine; Ala, alanine; Arg, arginine; Pro, proline; Cys, cysteine; Val, valine; Met, methionine; Ile, isoleucine; Leu, leucine; Tyr, tyrosine; Phe, phenylalanine; Lys, lysine; His, histidine; TFAAs, total FAAs; UFAAs, total Asp and Glu; SFAAs, total Thr, Ser, Gly, Ala, Arg, and Pro; BFAAs, total Val, Met, Ile, Leu, Phe, Tyr, Lys, and His. Hx, hypoxanthine; AMP, adenosine monophosphate; IMP, inosine monophosphate; GMP, guanosine monophosphate.

Toyohara, & Hayashi, 2003). Ser levels were significantly higher in S29 ($P < 0.05$), which may have caused it to have the highest sweetness value. Moreover, bitter FAAs showed a downward trend as the salinity decreased. The amino acid His is one of the most important bitter amino acids. Compared with the high-salinity group (S35 and S38), the His content in the low-salinity groups (S26 and S29) was reduced ($P < 0.05$). The reduction in the level of bitter amino acids would lead to a further decrease in *C. gigas* bitterness, which is consistent with the electronic tongue results.

Some FAAs, such as Thr, Ala, Lys, Asp, Glu, and Cys may be involved in the regulation of osmolality in Pacific oysters. Previous studies have reported that most FAAs show synchronous decreases from 2 h to 8 h during hypo-osmotic adaptation, and marked increases in Pro, Arg, Gly, Ala, and Tau were observed in hyperosmotic adaptation (Hosoi et al., 2003). Salinity can also improve the taste of seafood by changing the levels of certain FAAs (Frank et al., 2016).

In this study, after the depuration of oysters, the content of umami FAAs in S29 was found to be higher than that in other salinity groups, and the content of bitter FAAs was also reduced ($P < 0.05$) compared to the high salinity groups, further improving the taste quality of the *C. gigas* in this group. This finding was consistent with the results from the electronic tongue.

Analysis of 5′-nucleotides

ATP-related compounds could be degraded into flavor 5′-nucleotides (IMP, AMP, hypoxanthine (Hx), and GMP) (Yamaguchi, Yoshikawa,

Ikeda, & Ninomiya, 1971). The nucleotide content of the Pacific oysters is shown in Table 1. The IMP content significantly decreased after depuration at S26 and significantly increased at S29, S35, and S38 ($P < 0.05$). The AMP content of S29 was higher than that of S26 ($P < 0.05$), and AMP is a bitter taste inhibitor (Leksrisompong, Lopetcharat, Guthrie, & Drake, 2012). Moreover, the Hx content of S38 was remarkably higher than that of the other salinities ($P < 0.05$), and Hx is a bitter substance. This result was consistent with the electronic tongue results. There was a salinity fluctuation between the depuration and production areas of *C. gigas*, and this fluctuation could lead to the degradation of AMP and IMP to physiologically maintain balance. This implies that salinity stress could provoke a sharp increase in energy consumption. The main pathway of adenosine 5′-triphosphate (ATP) degradation in Pacific oysters is ATP → ADP → AMP → IMP → HxR → Hx (Yokoyama, Sakaguchi, Kawai, & Kanamori, 1992). It has been reported that adjusting seawater salinity can improve flavor nucleotides and enhance the taste quality of aquatic products, and our findings are consistent with these reports (Wang et al., 2018).

Organic acid analysis

Organic acids play an important role in the complex and unique taste of *C. gigas* (Chen et al., 2021b). Two types of organic acids (succinic acid and lactic acid) were detected in the Pacific oyster samples at different salinities (Table 1). The succinic acid content of the samples decreased significantly after depuration. The succinic acid content of S29 and S35 was significantly higher than that of S26, S32, and S38 ($P < 0.05$). There was no significant difference in lactic acid levels after depuration except for S32. The lactic acid content of S32 significantly decreased ($P < 0.05$). There were no significant differences at other salinities ($P > 0.05$). Lactic acid and succinic acid are the major flavor-enhancing acids in *C. gigas*, and they are produced during glycolysis (Chen et al., 2021a). Together, they make a large contribution to the taste characteristics of seafood. In addition, lactic acid may improve the buffer capacity and succinic acid has a sour taste. Furthermore, sodium succinate has a taste-enhancing effect, similar to that of glutamate. Similarly, studies have also reported that a change in seawater salinity could alter the production of organic acids and enhance the taste of seafood, which was consistent with our results (Dong, Hu, Chu, Zhao, & Tan, 2017).

EUC analysis

The EUC value reflects the synergistic interaction of MSG and flavor 5′-nucleotides (Feng et al., 2022). Table 1 shows that the EUC of the S29 samples was significantly higher than that of the samples depurated at other salinities ($P < 0.05$). However, the level of FAAs was not the highest in S29, which might be attributable to the difference in the relative umami coefficient. However, the trend was consistent with our electronic tongue results. Bi et al. (2021) reported that umami FAAs were highly correlated with the levels of energy substances such as ATP and AMP, and the EUC value was positively correlated with the energy level. Therefore, the umami taste of S29 was relatively higher than that of the samples depurated at the other salinities ($P < 0.05$). This may be because the energy level of *C. gigas* was higher at this salinity in this study. Moreover, the umami taste of S26 was lower than that of the other salinities tested ($P < 0.05$). This could be due to the fact that the salinity stress was greater at 26 g/L, resulting in *C. gigas* consuming more energy, leading to a lower energy state at this salinity. In conclusion, our results suggest that 29 g/L was the most effective salinity for depuration to improve oyster flavor.

Sensory evaluation

The taste profiles of *C. gigas* depurated at different salinities were evaluated using a sensory panel consisting of 10 individuals (Fig. S2). The effect of depuration salinity on the taste of *C. gigas* was also significant. As the depuration salinity of oyster samples increased, saltiness and bitterness significantly increased, while sweetness significantly decreased ($P < 0.05$). The umami taste of S29 was significantly higher than that of the other salinity groups. The Pacific oyster is normally enjoyed for its umami flavor and sweetness, while saltiness and bitterness are viewed as potentially harmful and generally disliked by consumers. Thus, it is important to optimize salinity content to achieve the balance of umami, sweetness, saltiness, and bitterness (Kingsley et al., 2015; Bi et al., 2021). The results showed that acceptable umami and sweetness levels of oysters were depurated by seawater with a salinity of 29 g/L. At the same time, the overall score of *C. gigas* at 29 g/L salinity was higher than that of the other groups, which was consistent with the results of instrument detection.

Odor component analysis of Pacific oyster at different salinities during depuration

Electronic nose analysis

The electronic nose was a sensor set imitating the human olfactory system (Loutfi, Coradeschi, Mani, Shankar, & Rayappan, 2015). The built-in gas sensor set had different response values to specific volatiles and used specific analysis methods to process the sensor response values, which in turn would distinguish different samples. Fig. 2A shows the LDA analysis diagram, which is a dimension reduction technique for supervised learning. The total contribution rate of the LDA analysis was 86.56 %, and the data points from the six groups of samples were distributed in different aggregation areas. These differences in distribution were significant. There was an overlap between S26, S29, and S32 (S35 and S38), suggesting that the odor profile of *C. gigas* was consistent with higher-salinity depuration or lower-salinity depuration. In addition, the distance between the normal group and the groups depurated at higher salinities was close to that of the Pro-depuration sample, suggesting that depuration at lower salinities has little impact on the odor of *C. gigas* depuration. The effect on odor was greatest for S26. Fig. 2B shows the response values of the electronic nose for the six groups of samples. This difference in odor profiles may be attributable to the depuration process itself, which results in changes in the levels of esters, aldehydes, ketones, and other VOCs. The response values of W1C and W1S changes were pronounced (Fig. 2B and Fig. S1), indicating that the change in odor during the depuration stage was mainly caused by nitrogen oxides and methyl compounds. The nitrogen oxide content increased after the depuration. The contents of methyl, alcohols, aldehydes, ketones, and long-chain alkanes decreased, especially with increased salinity depuration. However, the specific odor components require further analysis.

GC-IMS analysis

The analysis of VOC levels in the *C. gigas* depurated at different salinities was performed using GC-IMS, a non-targeted analytical strategy for determining VOC levels (Feng et al., 2022). The RI and DT values of VOCs were determined. The VOCs were identified by comparing their values with those in the GC × IMS library, and the results are listed by fingerprinting using the gallery plot (Fig. 2D). Notably, the same compound could detect small monomers and dimers and distinguish them from high-density monomer ions, such as 1-propanol, 2–5-dimethylfuran, and methanethiol.

Based on the VOC data, PCA (Fig. 2C) was used to distinguish the *C. gigas* depurated at different salinities. The scoring plot showed that the cluster of pre-depuration samples was far from that of the other samples, indicating that depuration had a significant effect on the VOCs present in *C. gigas*. A progressive change along PC1 was observed from the left to the right area of the plot as salinity increased, indicating that salinity had a consistent effect on VOCs in *C. gigas*. This finding is consistent with those of the electronic nose.

A total of 65 VOCs in the samples depurated at different salinities were identified. They fell into eight chemical classes and included 14 alcohols, 4 furans, 9 nitrogen-containing compounds, 3 sulfides, 9 aldehydes, 3 hydrocarbons, 9 ketones, 10 esters, and other compounds (Table 2). These findings are consistent with those of previous studies

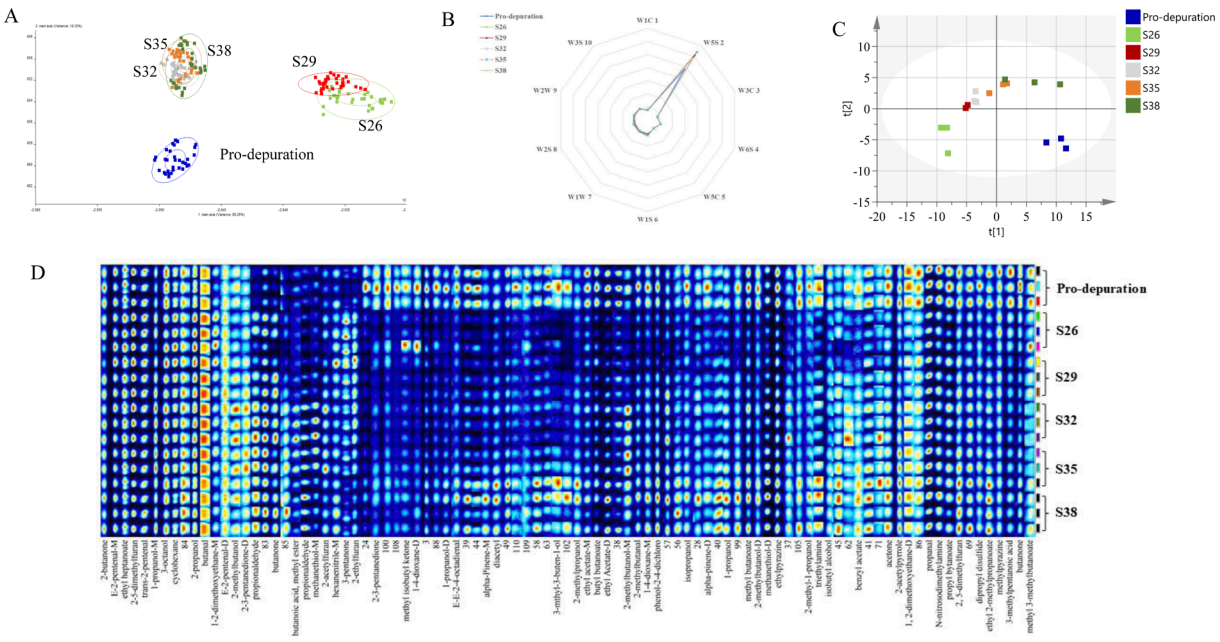

Fig. 2. Odor component analysis of Pacific oysters at different salinities during depuration. (A) Linear Discriminant Analysis (LDA) based on the electronic nose (E-nose) results; (B) Spider plot for the electronic nose sensory score based on the taste sensing system of the E-nose; (C) PCA based on gas chromatography-ion mobility spectrometry (GC-IMS); (D) Fingerprint spectra of VOCs in Pacific oyster based on GC-IMS. Each row represents a VOC. Each column represents one sample.

(Kawabe et al., 2019). The formation of VOCs is related to the degradation of lipids and proteins via non-enzymatic and enzymatic reactions (Tian et al., 2020). The highest levels of VOCs in the Pro-depuration samples indicated that microorganisms proliferated in the Pacific oyster before depuration, leading to a whole train of biochemical reactions that produced a large number of volatile components (Fig. 2D). After depuration, the microorganisms decreased, especially down-salinity depuration, which then led to the reduction of most VOCs in the Pacific oyster samples. The content of furans was increased, while alcohols, ethers, ketones, aldehydes, and sulfur were significantly decreased in the down-salinity depuration group, but there was no significant difference in the up-salinity depuration group, which was similar to the results of the electronic nose (Fig. 2D).

The largest peak area of VOCs was observed for alcohols, which had a mild characteristic odor and were one of the considerable VOCs in food (Nives, Sanja, Tibor, & Helga, 2016). They mainly originate from the reaction of polyunsaturated fatty acids catalyzed by lipoxygenase (Tian et al., 2020). In the depuration process at different salinities, the content of alcohols changed significantly, and was significantly higher after up-salinity depuration than after down-salinity depuration, and among them isopropanol and 2-methyl butanol were the highest. This might be due to the esterification of alcohols and acids after down-salinity depuration or the further reduction of alcohols to aldehydes. Down-salinity depuration inhibited the formation of alcohol, whereas up-salinity depuration promoted the formation of alcohol.

Aldehydes are more important VOCs than alcohols because of the lower odor thresholds of aldehydes, and these compounds have a strong impact on the aroma of marine products (Gemert, 2003; Hu et al., 2021). In the present study, the trend for aldehydes was similar to that for alcohols. The alcohol content after depuration at higher salinities was significantly higher than that after depuration at lower salinities. Of the aldehydes detected, propionaldehyde was present at the highest levels. The ketone trend was similar to that observed for the aldehydes and alcohols. Although ketones impart milk and sweet butter flavors, they can also enhance fishy flavors. Therefore, a high ketone content may impart a bad flavor to Pacific oysters. Aldehydes, ketones, and alcohols are mainly produced by the oxidative metabolism of proteins and fats. They are the main components of tastes and odors resulting from deterioration.

Furan compounds were the products in the early stage of the Maillard reaction and the precursors of nitrogen-containing heterocyclic compounds, such as alkyl pyrazine. They impart caramel flavor and baked food flavor to food and make a positive contribution to Pacific oyster flavor. After depuration, the furan content in each salinity group increased, especially in S29 and S32, which may lead to a better odor of Pacific oysters after depuration.

Overall, our results suggest that depuration salinity had a significant effect on the VOCs present in Pacific oysters. Decrease in depuration salinity led to the increased furan and decreased alcohol, ether, ketone, and aldehyde contents, which could make the flavor of oysters reach a level preferred by consumers. Combined with the changing trend of taste-related substances following depuration, a salinity of 29 g/L was found to be the best salinity for oysters. In summary, the depuration salinity can be adjusted to optimize the oyster flavor, which can promote the development of the raw oyster industry.

Chemometric analysis

Flavor quality analysis of Pacific oyster after depuration

Based on the above conclusions, depuration had an impact on the flavor of Pacific oysters. Here, OPLS-DA, a supervised analysis method, was used to screen the markers of flavor changes after depuration, and the effectiveness of this model is shown in Fig. 3A. Pro-depuration and depuration samples were well separated in the OPLS-DA model. For potential marker discovery, variable importance projection parameter value (VIP) >1.0 was recognized as a marker (Zhang et al., 2019), and the results are shown in Fig. 3B. Thirty-four substances were screened, including aldehydes, ketones, esters, FAAs, alanine, and glutamate, which could be used as markers of depuration in the Pacific oysters.

SUS-plot analysis of Pacific oysters at different depuration salinities

As shown in these results (Fig. 3C), higher salinities (S35 and S38) and lower salinities (S26 and S29) during depuration had the same impact on *C. gigas* flavor characteristics. The loading plot included three variables that were difficult to interpret using pairwise OPLS-DA. Therefore, SUS-plots were used to synthesize the loadings of the two

Table 2
GC-IMS integration parameters of VOCs in *Crassostrea gigas* depurated at different salinities.

Nos.	Compound	CAS#	Formula	MW	RI	Rt (s)	Dt [RIP relative]
	Alcohols						
1	2-Propanol-D	C67630	C3H8O	60.1	881.5	285.166	1.1703
2	1-Propanol-M	C71238	C3H8O	60.1	1070.1	598.320	1.1077
3	3-Octanol	C589980	C8H18O	130.2	994.8	451.191	1.4068
4	2-Propanol-M	C67630	C3H8O	60.1	928.7	343.254	1.1785
5	2-methylbutanol	C137326	C5H12O	88.1	1210.7	1039.257	1.2243
6	1-propanol-D	C71238	C3H8O	60.1	1025.9	514.278	1.2525
7	3-Methyl-3-buten-1-ol	C763326	C5H10O	86.1	720.6	149.733	1.5091
8	2-methylpropanol	C78831	C4H10O	74.1	637.4	110.393	1.1774
9	2-methylbutanol-M	C137326	C5H12O	88.1	734.0	157.579	1.2279
10	Isopropanol	C67630	C3H8O	60.1	911.1	320.216	1.1816
11	1-Propanol	C71238	C3H8O	60.1	1051.6	556.338	1.1031
12	2-Methylbutanol-D	C137326	C5H12O	88.1	1182.9	931.921	1.2313
13	2-methyl-1-propanol	C78831	C4H10O	74.1	1085.2	634.771	1.1641
14	isobutyl alcohol	C78831	C4H10O	74.1	1048.1	548.756	1.1769
	Furans						
15	2–5-Dimethylfuran-M	C625865	C6H8O	96.1	946.4	368.049	1.3267
16	2-Acetylfuran	C1192627	C6H6O2	110.1	1069.1	595.571	1.4460
17	2-ethylfuran	C3208160	C6H8O	96.1	963.3	393.264	1.3067
18	2–5-Dimethylfuran-D	C625865	C6H8O	96.1	708.2	142.954	1.3572
	N-containing compounds						
19	hexanenitrile-D	C628739	C6H11N	97.2	885.3	289.483	1.5841
20	3-Butenenitrile-M	C109751	C4H5N	67.1	630.6	107.760	1.1301
21	1–2-Dimethoxyethane-M	C110714	C4H10O2	90.1	666.9	139.785	1.1124
22	hexanenitrile-M	C628739	C6H11N	97.2	889.5	291.511	1.2628
23	ethylpyrazine	C13925003	C6H8N2	108.1	928.3	341.983	1.5187
24	Triethylamine	C121448	C6H15N	101.2	721.2	150.023	1.4631
25	2-Acetylpyrrole	C1072839	C6H7NO	109.1	1074.6	632.455	1.0971
26	*N*-nitroso dimethylamine	C62759	C2H6N2O	74.1	755.6	171.130	1.2553
27	Methylpyrazine	C109080	C5H6N2	94.1	1238.2	1270.352	1.1002
	Sulfur compounds						
28	Methanethiol-M	C74931	CH4S	48.1	711.2	158.379	1.036
29	Methanethiol-D	C74931	CH4S	48.1	646.3	132.453	1.0423
30	dipropyl disulfide	C629196	C6H14S2	150.3	1098.5	668.974	1.4757
	Aldehydes						
31	*trans*-2-pentenal	C1576870	C5H8O	84.1	757.3	172.264	1.1097
32	Butanal	C123728	C4H8O	72.1	869.9	272.642	1.2243
33	E-2-pentenal-D	C1576870	C5H8O	84.1	1169.5	884.023	1.3579
34	Propionaldehyde	C123386	C3H6O	58.1	800.8	211.550	1.1727
35	Propionaldehyde-D	C123386	C3H6O	58.1	799.4	210.489	1.3923
36	E-E-2–4-octadienal	C30361285	C8H12O	124.2	1108.4	695.503	1.2634
37	2-Methylbutanal	C96173	C5H10O	86.1	930.9	346.329	1.4024
38	Propanal	C123386	C3H6O	58.1	746.6	176.569	1.0342
	hydrocarbon						
39	Cyclohexane	C110827	C6H12	84.2	724.9	165.003	1.0782
40	alpha-Pinene-M	C80568	C10H16	136.2	1012.8	477.645	1.2213
41	alpha-Pinene-D	C80568	C10H16	136.2	1006.5	473.778	1.2848
	Ketones						
42	2-Butanone	C78933	C4H8O	72.1	932.7	348.666	1.0613
43	2–3-Pentanedione-D	C600146	C5H8O2	100.1	1068.7	594.953	1.2267
44	butanone-M	C78933	C4H8O	72.1	962.4	391.959	1.2547
45	3-Pentanone	C96220	C5H10O	86.1	696.2	151.583	1.1124
46	2–3-pentanedione	C600146	C5H8O2	100.1	1053.5	560.434	1.2206
47	Methyl isobutyl ketone	C108101	C6H12O	100.2	733.8	157.462	1.1837
48	diacetyl	C431038	C4H6O2	86.1	971.9	406.736	1.1728
49	acetone	C67641	C3H6O	58.1	816.2	223.232	1.1101
50	butanone-D	C78933	C4H8O	72.1	917.8	328.961	1.2477
	Ester						
51	ethyl heptanoate	C106309	C9H18O2	158.2	1095.3	660.458	1.4089
52	Butanoic acid, methyl ester	C623427	C5H10O2	102.1	715.8	160.535	1.1402
53	Ethyl acetate-M	C141786	C4H8O2	88.1	911.5	320.814	1.0909
54	Butyl butanoate	C109217	C8H16O2	144.2	994.3	450.088	1.8184
55	Ethyl Acetate-D	C141786	C4H8O2	88.1	895.3	301.033	1.3355
56	Methyl butanoate	C623427	C5H10O2	102.1	952.1	376.315	1.1465
57	Benzyl acetate	C140114	C9H10O2	150.2	1163.1	861.757	1.3271
58	propyl bytanoate	C105668	C7H14O2	130.2	896.2	299.336	1.6915
59	ethyl 2-methylpropanoate	C97621	C6H12O2	116.2	763.4	176.347	1.1995

(*continued on next page*)

Table 2 (*continued*)

Nos.	Compound	CAS#	Formula	MW	RI	Rt (s)	Dt [RIP relative]
60	methyl 3-methylbutanoate	C556241	C6H12O2	116.2	1030.6	524.532	1.5432
	other						
61	1–4-Dioxane-D	C123911	C4H8O2	88.1	1069.6	597.132	1.3242
62	1–4-dioxane-M	C123911	C4H8O2	88.1	1093.6	685.777	1.1187
63	1–2-Dimethoxyethane-D	C110714	C4H10O2	90.1	669.3	123.799	1.3071
64	Phenol-2–4-dichloro	C120832	C6H4Cl2O	163	1162.9	861.337	1.1968
65	3-Methylpentanoic acid	C105431	C6H12O2	116.2	961.2	391.934	1.6002

MW, molecular mass; RI, retention index; Rt, retention time; Dt, drift time; D, means dimer; M, means monomer.

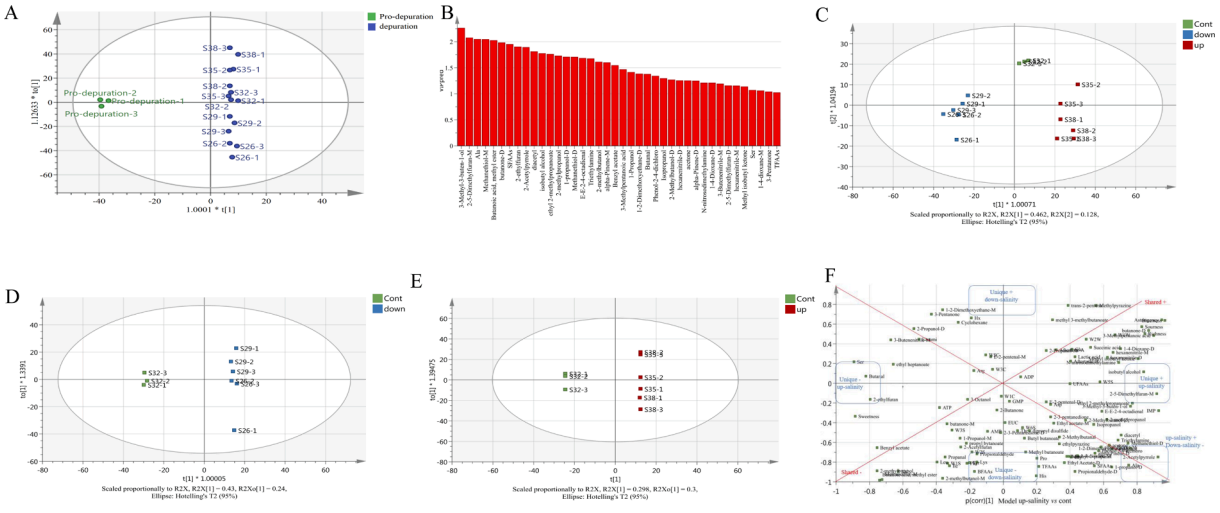

Fig. 3. Chemometric analysis of *Crassostrea gigas* at different salinities during depuration. (A) Score plots of the independent orthogonal partial least squares (OPLS-DA) of flavor analysis of *C. gigas* after depuration; (B) VIP plot of the independent OPLS-DA model; (C) OPLS-DA of flavor components of *C. gigas* for higher-salinity depurations and lower-salinity depurations; (D) OPLS-DA of flavor components of *C. gigas* for lower-salinity depurations; (E) OPLS-DA of flavor components of Pacific oysters for higher-salinity depurations; (F) SUS-plot analysis of *C. gigas* depurated at different salinities.

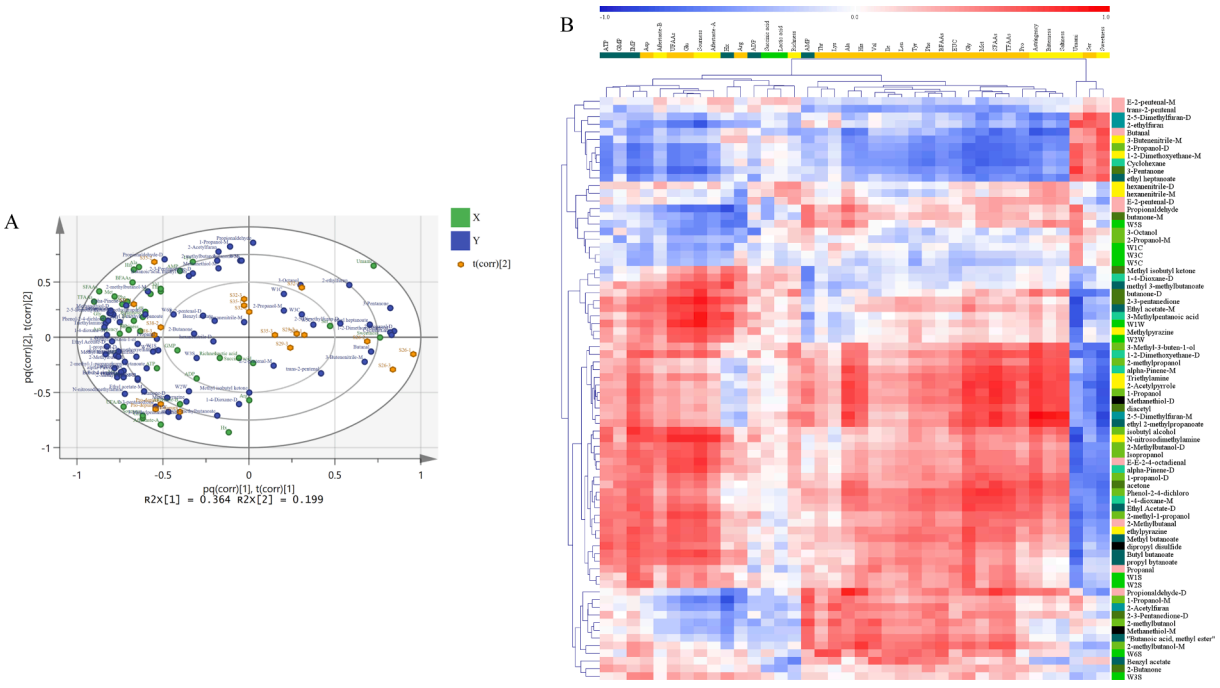

Fig. 4. (A) Bidirectional orthogonal partial least squares (O2PLS) overview biplot of taste and odor in *Crassostrea gigas*; (B) Heatmap of the correlation coefficient matrix between taste and odor traits of *C. gigas* produced using O2PLS modeling.

OPLS-DA models and screen the flavor change substances caused by salinity stress (Boccard et al., 2011). The SUS-plot in Fig. 3F shows the correlation between the predictive component |*p(corr)*| of the higher-salinity depurations (S35 and S38) *vs* Cont. (S32) (Model 1 in Fig. 3E) on the x-axis and lower-salinity depurations (S26 and S29) *vs* Cont. (S32) (Model 2 in Fig. 3D) on the y axis (Boccard et al., 2011). Ethyl 2-methyl propanoate, 2–5-dimethylfuran-M, and isobutyl alcohol were higher in the higher-salinity depurations, and 2-ethylfuran, butanal, and Ser were lower in the higher-salinity depurations than in the lower-salinity depurations. His, BFAAs, Lys, Pro, TFAAs, and propionaldehyde levels were lower in the lower-salinity depurations than in the higher-salinity depuration. This model showed that the changes in the "shared structure" in the same direction for both higher-salinity and lower-salinity depurations were in methylpyrazine, Glu, lactic acid, W2W, succinic acid, W1W, Val, methanethiol-M, butanoic acid, methyl ester, 2-methyl butanol, and benzyl acetate. Other identified flavor components such as 2-acetylpyrrole, Ala, 1-propanol-D, 1-2-dimethoxyethane-D, methanethiol-D, and acetone were also the "shared flavor components" in the opposite direction for higher-salinity and lower-salinity depurations. These markers could be used to identify high- or low-salinity depurations and further clarify the regulatory mechanisms of salinity during the depuration process.

The relationship between the taste and odor of C. gigas

To investigate the relationship between the taste and odor of *C. gigas*, an O2PLS model was established. The O2PLS biplot can provide a visual representation of the two data sources and indicate several taste-related compounds that co-vary with odor-related compounds (Fig. 4A) (Zang et al., 2020). The relationship between the variables (positive or negative correlations) is characterized by distance and direction. On the left side of the O2PLS biplot, AMP, His, and Ala were positively associated with odorous compounds (2-methyl butanol, propionaldehyde-D, and alpha-pinene-M). O2PLS also provided the correlation coefficient matrix between the taste and odor traits of *C. gigas* and this is displayed using a heatmap (Fig. 4B; detailed data are shown in Tab. S2). Among the odor compounds in the oyster samples, butanal, acetone, alpha-pinene-M, diacetyl, triethylamine, 1-2-dimethoxyethane, methanethiol, 2-acetylpyrrole, 1-propanol, ethyl 2-methylpropanoate, and 2-5-dimethylfuran were considered to have a strong correlation ($|r| > 0.7$) with the sweetness of *C. gigas*. The taste-related compounds 2-5-dimethylfuran, ethyl 2-methylpropanoate, 2-acetylpyrrole, triethylamine, methanethiol, diacetyl, 1-propanol, acetone, and 2-methylpropanol were identified as the most relevant to astringency because they were strongly correlated with $|r| > 0.7$, and bitterness was moderately correlated with the six odor compounds.

O2PLS is a two-way multivariate statistical analysis method that has been widely used to study the correlation between two types of data, such as sensory characteristics and metabolites, volatile characteristics, and flavor characteristics (Iijima et al., 2016; Wang et al., 2020; Zang et al., 2020). The mathematical correlations between the taste and odor traits of *C. gigas* have been established, and future studies should focus on the biological relationships between these two parameters.

In summary, markers of oyster flavor substances after depuration were screened using multivariate data analysis, and the correlation coefficients of taste traits and odor traits were established. These markers can be used to detect changes in oyster quality after depuration.

Conclusion

This study suggests that 29 g/L is the optimum salinity for the depuration of *C. gigas.* With a decrease in salinity, bitter FAAs substances in *C. gigas* significantly decrease. The EUC was found to be the highest at a salinity of 29 g/L, which was consistent with the electronic tongue results. Moreover, the gallery plot diagram of the VOCs showed that the highest peak area of VOCs was found before depuration; however, the content of aldehydes and ketones in the odor was reduced, whereas furan levels increased after lower-salinity depurations. Furthermore, 34 markers of *C. gigas* were selected for depuration by OPLS-DA, including aldehydes, ketones, esters, FAAs, alanine, and glutamate, which were further classified by the SUS-plot of higher-salinity (S35 and S38) or lower-salinity (S26 and S29) depuration. Finally, there is a close correlation between odor and taste substances through O2PLS analysis. This study provides a theoretical basis for salinity selection to maintain the best flavor in Pacific oysters. However, further studies are needed to explore the possible molecular mechanisms underlying flavor synthesis in Pacific oysters.

Declaration of Competing Interest

The authors declare that they have no known competing financial interests or personal relationships that could have appeared to influence the work reported in this paper.

Data availability

Data will be made available on request.

Acknowledgments

This work was supported by the Fundamental Research Funds for the Central Universities (202161027), and earmarked fund for Modern Agro-industry Technology Research System (CARS-49).

Author contributions

Li-pin Chen, Hao-hao Shi, Chang-hu Xue, and Zhao-jie Li designed the study. Li-pin Chen, Qi Wang, and Yong Xue performed the research including data analysis and literature search. Li-pin Chen, Fan-qian-hui Yu, Yuming Wang and Hong-wei Zhang wrote and revised the manuscript.

Appendix A. Supplementary data

Supplementary data to this article can be found online at https://doi.org/10.1016/j.fochx.2022.100485.

References

Abdul Ghani, Z. D. F., Husin, J. M., Rashid, A. H. A., Shaari, K., & Chik, Z. (2016). Biochemical studies of Piper betle L leaf extract on obese treated animal using 1H-NMR-based metabolomic approach of blood serum samples. *Journal of Ethnopharmacology, 194*, 690–697.

Anacleto, P., Maulvault, A. L., Nunes, M. L., Carvalho, M. L., Rosa, R., & Marques, A. (2015). Effects of depuration on metal levels and health status of bivalve molluscs. *Food Control, 47*, 493–501.

Bagenda, D. K., Nishikawa, S., Kita, H., Kinai, Y., Terai, S., Kato, M., et al. (2019). Impact of feeding on oyster depuration efficacy under conditions of high salinity and low temperature. *Aquaculture, 500*, 135–140.

Bi, S., Chen, L., Sun, Z., Wen, Y., Xue, Q., Xue, C., et al. (2021). Investigating influence of aquaculture seawater with different salinities on non-volatile taste-active compounds in Pacific oyster (*Crassostrea gigas*). *Journal of Food Measurement & Characterization, 15*(2), 2078–2087.

Boccard, J., Badoud, F., Grata, E., Ouertani, S., Hanafi, M., Mazerolles, G., et al. (2011). A steroidomic approach for biomarkers discovery in doping control. *Forensic Science International, 213*(1–3), 85–94.

Chen, L., Yu, F., Shi, H., Wang, Q., Xue, Y., Xue, C., et al. (2021a). Effect of salinity stress on respiratory metabolism, glycolysis, lipolysis, and apoptosis in Pacific oyster (*Crassostrea gigas*) during depuration stage. *Journal of the Science of Food and Agriculture, 102*, 2003–2011.

Chen, L., Yu, F., Sun, S., Liu, X., Sun, Z., Cao, W., et al. (2021b). Evaluation indicators of *Ruditapes philippinarum* nutritional quality. *Journal of Food Science and Technology, 58*(8), 2943–2951.

Chen, L., Zhang, H., Zhang, X., Yu, F., Zhang, F., Xue, C., et al. (2020). Identification of potential peptide markers for the shelf-life of Pacific oysters (*Crassostrea gigas*) during anhydrous preservation via mass spectrometry-based peptidomics. *LWT, 134*, Article 109922.

Cochet, M., Brown, M., Kube, P., Elliott, N., & Delahunty, C. (2015). Understanding the impact of growing conditions on oysters: A study of their sensory and biochemical characteristics. *Aquaculture Research, 46*(3), 637–646.

Dong, W., Hu, R., Chu, Z., Zhao, J., & Tan, L. (2017). Effect of different drying techniques on bioactive components, fatty acid composition, and volatile profile of robusta coffee beans. *Food Chemistry, 234*, 121–130.

Duan, Z., Dong, S., Dong, Y., & Gao, Q. (2021). Geographical origin identification of two salmonid species via flavor compound analysis using headspace-gas chromatography-ion mobility spectrometry combined with electronic nose and tongue. *Food Research International, 145*, Article 110385.

Duan, Z., Dong, S., Sun, Y., Dong, Y., & Gao, Q. (2021). Response of Atlantic salmon (*Salmo salar*) flavor to environmental salinity while culturing between freshwater and seawater. *Aquaculture, 530*, Article 735953.

FAO (2020). *The State of World Fisheries and Aquaculture 2020. Sustainability in Action*. Rome. https://doi.org/10.4060/ca9229en.

Feng, X., Ng, V. K., Mikś-Krajnik, M., & Yang, H. (2017). Effects of fish gelatin and tea polyphenol coating on the spoilage and degradation of myofibril in fish fillet during cold storage. *Food and Bioprocess Technology, 10*, 89–102.

Feng, Y., Xin, G., Wei, Y., Xu, H., Sun, L., Hou, Z., et al. (2022). Comparison of the umami taste and aroma of dried *Suillus* granulatus packed using four different packaging methods. *Food Chemistry, 366*, Article 130570.

Frank, D. C., Ball, A. J., Hughes, J. M., Piyasiri, U., Stark, J., Watkins, P., et al. (2016). Sensory and flavor chemistry characteristics of australian beef; the influence of intramuscular fat, feed and breed. *Journal of Agricultural & Food Chemistry, 4299*.

Gemert, L.J.V. Compilations of odour threshold values in air, water and other media. 2003.

Hosoi, M., Kubota, S., Toyohara, M., Toyohara, H., & Hayashi, I. (2003). Effect of salinity change on free amino acid content in Pacific oyster. *Fisheries Science, 69*(2), 395–400.

Hu, M., Wang, S., Liu, Q., Cao, R., & Xue, Y. (2021). Flavor profile of dried shrimp at different processing stages. *LWT, 146*, Article 111403.

Huang, X., Qi, L., Fu, B., Chen, Z., Zhang, Y., Du, M., et al. (2019). Flavor formation in different production steps during the processing of cold-smoked Spanish mackerel. *Food Chemistry, 286*, 241–249.

Iijima, Y., Iwasaki, Y., Otagiri, Y., Tsugawa, H., Sato, T., Otomo, H., et al. (2016). Flavor characteristics of the juices from fresh market tomatoes differentiated from those from processing tomatoes by combined analysis of volatile profiles with sensory evaluation. *Bioscience, Biotechnology, and Biochemistry, 80*(12), 2401–2411.

Kawabe, S., Murakami, H., Usui, M., & Miyasaki, T. (2019). Changes in volatile compounds of living Pacific oyster *Crassostrea gigas* during air-exposed storage. *Fisheries Science., 85*, 747–755.

Kingsley, D. H., Duncan, S. E., Granata, L. A., Salinas-Jones, A., Flick, G. J., Bourne, D. M., et al. (2015). High-pressure processing with hot sauce flavouring enhances sensory quality for raw oysters (*Crassostrea virginica*). *International Journal of Food Science & Technology, 50*(9), 2013–2021.

Leksrisompong, P., Lopetcharat, K., Guthrie, B., & Drake, M. A. (2012). Descriptive analysis of carbonated regular and diet lemon-lime beverages. *Journal of Sensory Studies, 27*(4), 247–263.

Li, S., Tian, Y., Jiang, P., Lin, Y., Liu, X., & Yang, H. (2021). Recent advances in the application of metabolomics for food safety control and food quality analyses. *Critical Reviews in Food Science and Nutrition, 61*(9), 1448–1469.

Loutfi, A., Coradeschi, S., Mani, G. K., Shankar, P., & Rayappan, J. B. B. (2015). Electronic noses for food quality: A review. *Journal of Food Engineering, 144*, 103–111.

Nives, M. R., Sanja, V., Tibor, J., & Helga, M. (2016). Characterization of volatile compounds, physico-chemical and sensory characteristics of smoked dry-cured ham. *Journal of Food Science and Technology, 53*(11), 4093–4105.

Tian, X., Li, Z. J., Chao, Y. Z., Wu, Z. Q., Zhou, M. X., Xiao, S. T., et al. (2020). Evaluation by electronic tongue and headspace-GC-IMS analyses of the flavor compounds in dry-cured pork with different salt content. *Food Research International, 137*, Article 109456.

Wang, H., Wei, H., Tang, L., Lu, J., Mu, C., & Wang, C. (2018). A proteomics of gills approach to understanding salinity adaptation of Scylla paramamosain. *Gene, 677*, 119–131.

Wang, X., Jiang, G., Kebreab, E., Li, J., Feng, X., Li, C., et al. (2020). 1H NMR-based metabolomics study of breast meat from Pekin and Linwu duck of different ages and relation to meat quality. *Food Research International, 133*, Article 109126.

Xu, X., Sun, C., Liu, B., Zhou, Q., Xu, P., Liu, M., … Jiang, Q. (2022). Flesh flavor of red swamp crayfish (*Procambarus clarkii Girard*, 1852) processing by GS-IMS and electronic tongue is changed by dietary animal and plant protein. *Food Chemistry, 373*, Article 131453.

Yamaguchi, S., Yoshikawa, T., Ikeda, S., & Ninomiya, T. (1971). Measurement of the relative taste intensity of some l-α-amino acids and 5'-nucleotides. *Journal of Food Science, 36*(6), 846–849.

Yao, L., Jiang, Y., Wang, L., Zhai, M., Guo, Y., Zhu, W., Ning, J., Zuo, H., & Lu, L (2018). Guidelines for the sensory evaluation of aquatic products. Chinese national standard, GB/T 37062-2018 (In Chinese).

Yokoyama, Y., Sakaguchi, M., Kawai, F., & Kanamori, M. (1992). Changes in concentration of ATP-related compounds in various tissues of oyster during ice storage. *Nippon Suisan Gakkaishi, 58*(11), 2125–2136.

Yuasa, M., Kawabeta, K., Eguchi, A., Abe, H., Yamashita, E., Koba, K., et al. (2018). Characterization of taste and micronutrient content of rock oysters (*Crassostrea nippona*) and Pacific oysters (*Crassostrea gigas*) in Japan. *International Journal of Gastronomy & Food Science, 13*, 52–57.

Zang, J., Xu, Y., Xia, W., Regenstein, J. M., Yu, D., Yang, F., et al. (2020). Correlations between microbiota succession and flavor formation during fermentation of Chinese low-salt fermented common carp (*Cyprinus carpio L.*) inoculated with mixed starter cultures. *Food Microbiology, 90*, Article 103487.

Zhang, H., Zhang, X., Zhao, X., Xu, J., Lin, C., Jing, P., et al. (2019). Discrimination of dried sea cucumber (*Apostichopus japonicus*) products from different geographical origins by sequential windowed acquisition of all theoretical fragment ion mass spectra (SWATH-MS)-based proteomic analysis and chemometrics. *Food Chemistry, 274*, 592–602.

Zhang, L., Yin, M., Zheng, Y., Tao, N., Wu, X., & Wang, X. (2021). Short-term rearing in brackish water regulates the taste-related metabolites of abdomen muscle for adult male *Eriocheir sinensis*. *LWT, 142*, Article 110898.

Zhang, L., Yin, M., Zheng, Y., Xu, C., Tao, N., Wu, X., et al. (2021). Brackish water improves the taste quality in meat of adult male *Eriocheir sinensis* during the postharvest temporary rearing. *Food Chemistry, 343*, Article 128409.

Zhao, X., Chen, L., Wongmaneepratip, W., He, Y., Zhao, L., & Yang, H. (2021). Effect of vacuum impregnated fish gelatin and grape seed extract on moisture state, microbiota composition, and quality of chilled seabass fillets. *Food Chemistry, 354*, Article 129581.

Zhao, X., Wu, J. E., Chen, L., & Yang, H. (2019). Effect of vacuum impregnated fish gelatin and grape seed extract on metabolite profiles of tilapia (*Oreochromis niloticus*) fillets during storage. *Food Chemistry, 293*, 418–428.